Exp Fluids (2011) 51:65–74
DOI 10.1007/s00348-010-1033-7

RESEARCH ARTICLE

An experimental study of pulsed micro-flows pertinent to continuous subcutaneous insulin infusion therapy

Bin Wang · Ayodeji Demuren · Eric Gyuricsko · Hui Hu

Received: 15 February 2010 / Revised: 19 August 2010 / Accepted: 16 December 2010 / Published online: 31 December 2010

Abstract An experimental study was conducted to investigate the unsteady micro-flow driven by an insulin pump commonly used in continuous subcutaneous insulin infusion (CSII) therapy. A microscopic particle image velocimetry (PIV) system was used to characterize the transient behavior of the micro-flow upon the pulsed excitation of the insulin pump in order to elucidate the underlying physics for a better understanding of the microphysical process associated with the insulin delivery in CSII therapy. The effects of air bubbles entrained inside the micro-sized CSII tubing system on the insulin delivery process were also assessed based on the micro-PIV measurements. While most solutions to insulin occlusion-related problems are currently based on clinical trials, the findings derived from the present study can be used to provide a better guidance for the troubleshooting of insulin occlusion in CSII therapy.

1 Introduction

In recent years, there has been a surge in the use of continuous subcutaneous insulin infusion (CSII), also known as insulin pump therapy, as opposed to the more traditional use of multiple daily injection (MDI) therapy to treat type 1 diabetes (Alemzadeh et al. 2004; Shalitin and Phillip 2008). CSII delivers insulin to the person with diabetes continuously simulating the natural internal secretion of insulin from the pancreas (Rossetti et al. 2008). Major advantages of CSII over MDI include the following: more precise amounts of insulin can be delivered as needed than by use of a syringe; better control over background or 'basal' insulin dosage can be gained to meet all the body's nonfood-related insulin needs; insulin pump software automatically determines the 'bolus' infusion dosages based on expected carbohydrate intake and current blood sugar level (Bruttomesso et al. 2009).

During CSII, insulin must travel from the insulin pump's reservoir, through various lengths of micron-sized capillary tubing, infusion set, and finally via a catheter to the patient's subcutaneous space, without occlusion. This must occur accurately, regardless of ambient temperature, the activity level of the patient, or low basal infusion rates. Young children require very small amounts of insulin to manage their diabetes. This results in a very slow rate of continuous insulin infusion, often on the order of 1.0 μl (or 0.1 units of insulin) per hour. As a consequence of this slow infusion rate, occlusion to insulin flow can, and often does, occur. There is anecdotal evidence, supported by results of comprehensive surveys (Hartman 2008; Weissberg-Benchell et al. 2007), that the actual insulin delivery dosage might fall short of the pre-programmed value at relatively low flow rates, leading to reduced glycemic control. Occlusion of insulin delivery, if not detected and immediately treated, may result in severe, sustained hyperglycemia, or diabetic ketoacidosis (DKA). Frequent occlusive episodes may result in suboptimal glycemic control, elevated hemoglobin A1C values, and an increased risk of long-term complications of diabetes (Weissberg-

B. Wang · H. Hu (✉)
Aerospace Engineering Department, Iowa State University, Ames, IA 50011, USA
e-mail: huhui@iastate.edu

A. Demuren
Mechanical Engineering Department, Old Dominion University, Norfolk, VA 23529, USA

E. Gyuricsko
Children's Hospital of The King's Daughters, Eastern Virginia Medical School, Norfolk, VA 23501, USA

Benchell et al. 2007). Case studies presented by Poulsen et al. (2005) and Wolpert et al. (2002) suggest that delivery failure may be caused by precipitation of insulin within the infusion set. There are also speculations that the flow of insulin through the infusion set may be reduced or impaired by air bubbles entrained in the micron-sized tubing system of the infusion set during the typical 3- to 5-day operation between refills. To date, this is still a subject of much debate.

Currently, most solutions to insulin occlusion-related problems are based on clinical trials. It is of great value to elucidate underlying physics of insulin infusion process, from the pump action to the catheter delivery, and from a fluid dynamics perspective, in order to provide a better guidance for troubleshooting. In this regard, Demuren and Doane (2007) and Demuren et al. (2009) carried out pioneer studies on the accuracy of insulin delivery by different pump types (Paradigm 511/512/712, Animas, and Omnipod) over a wide range of flow rates from 0.1 to 2.0 units per hour (U/H). They found that the operation of the insulin pumps was anything but continuous. The insulin pumps use stepper motors that operate for only a short moment each time. The screw pumps to which they are attached deliver 0.1 unit (i.e., 1.0 μl) each time. The consequence is that for an infant with a prescribed basal dosage of 0.1 U/H, an insulin pump only operates once per hour. If the flow was occluded in any way, it would have to wait another hour for the next delivery opportunity. On the other hand, an adult, with a typical basal dosage of 1.0 U/H, only have to wait for 6 min for the next delivery opportunity. Thus, dangers from occlusive events are much more severe in infants and young children than in adults. They also found that the unsteady flow features are the same for any insulin pumping pulses irrespective of nominal basal dosage; they merely occur more frequently at higher programmed dosages. Demuren et al. (2009) also observed air bubble formation in the reservoir and injection in infusion sets during experiments, but were unable to characterize the extent and overall impact of air bubbles on insulin delivery in CSII therapy.

It should be noted that the work of Demuren and Doane (2007) and Demuren et al. (2009) was based on bulk flow rate measurements, it is quite difficult, if not impossible, to extract detailed information (i.e., temporal-and-spatially-resolved flow field measurement results) to quantify the transient behavior of the unsteady micro-flows inside the micro-sized insulin infusion sets from the bulk flow rate measurements. In the present study, a microscopic particle image velocimetry (micro-PIV) system is used to conduct detailed flow velocity field measurements to characterize the transient behavior of the unsteady micro-flows inside a micro-sized capillary infusion tubing system commonly used in CSII therapy. The effects of the air bubbles entrained into the micro-sized tubing system on the insulin delivery process are also assessed based on the detailed micro-PIV measurements. The objective of the study is to elucidate underlying physics for a better understanding of the microphysical process associated with the insulin delivery in order to provide a better guidance for the troubleshooting of insulin occlusion in CSII therapy.

2 Experimental setup and micro-PIV measurements

Figure 1 shows the schematic of the experimental setup used in the present study. A Medtronic MiniMed Paradigm 512 insulin pump was used to drive the flow passing through a standard Paradigm Quick-Set infusion set. The inner diameter (I.D.) of the infusion tubing of the Paradigm Quick-Set infusion set is about 350 μm. The insulin pump uses a program-controlled proprietary stepper motor turning a captive lead screw that pushes the plunger on the reservoir and delivers insulin in discrete 0.1-unit increments (1.0 μl) per pulse cycle. In the present study, the insulin pump was set to operate in basal mode with the flow rate of 2.0 U/H (i.e., 20 μl per hour).

A micro-PIV system was used in the present study to conduct detailed flow velocity field measurements to characterize the transient behavior of the unsteady micro-flows driven by the insulin pump. The micro-PIV technique, which is the most commonly used tool for in situ imaging of micro-flows, derives flow velocity vectors by observing the motions of tracer particles seeded in the flows (Santiago et al. 1998; Meinhart et al. 1999; Olsen and Bourdon 2003, Park et al. 2003; Kinoshita et al. 2007). It should be noted that while microchannel flows driven by pressure force (Santiago et al. 1998, Li and Olsen 2006), capillary effects (Prins et al. 2001; Gallardo et al. 1999), electric fields (Kim et al. 2002), or centrifugal forces (Johnson et al. 2001) have been studied extensively in recent years majority of those previous studies were conducted with the micro-flows in steady state and driven by steady (time-invariant) compelling forces. In the present study, the micro-flow inside the micro-sized CSII tubing system was driven by a pulsed insulin pump, which have not been fully explored before.

It should be noted that since the circular tygon tubing of the standard Paradigm Quick-Set infusion set is only semi-transparent it is very difficult, if not impossible, to conduct quantitative micro-PIV measurements to quantify the micro-flow inside the micro-sized, circular tygon tubing. As shown in Fig. 1, a 38-mm-long transparent microchannel (Translume Corp.) with cross-sectional dimension of 300 × 300 μm (i.e., having almost the same area as the circular tygon tubing) was used in the present study to act as a part of the CSII tubing system for the micro-PIV

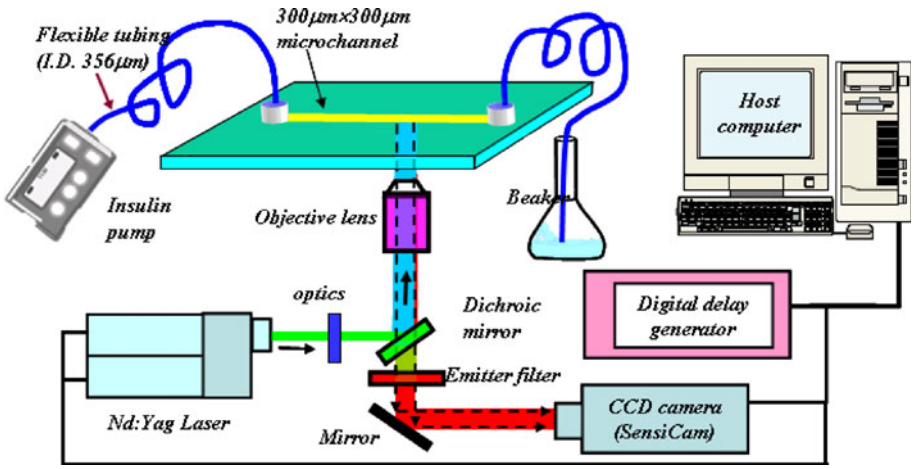

Fig. 1 Experimental setup

measurements. For simplicity, purified DI water, instead of insulin, was used as the working fluid in the present study. It should also be noted that when the catheter is inserted to a patient the CSII infusion system would face a pressure fluctuation due to the patient's blood pressure. Such pressure fluctuations were not simulated in the present experimental setup. The effects of the pressure fluctuations due to the patient's blood pressure on the insulin delivery process will be studied in the future.

In the present study, Nile red fluorescent FluoSpheres® beads (535/575 nm, ~1 μm in diameter) premixed in the reservoir were used as the tracers for the micro-PIV measurements. Illumination was provided by a double-pulsed Nd:YAG laser (NewWave) adjusted on the second harmonic and emitting two pulses of ~2 mJ per pulse at the wavelength of 532 nm. The repetition rate of the double-pulsed laser illumination was 10 Hz. Upon the pulsed excitations of the green laser beam at 532 nm, the tracer particles seeded in the micro-flows will emit fluorescent light with an emission peak at 575 nm. The fluorescence from the exited trace particles, which passes through a 10× objective lens (NA = 0.4, depth of field about 5.0 μm), a long pass optic filter (580 nm long pass filter), and the optical path inside an inverted microscope (Leica DM-IL), was recorded by a 12-bit high-resolution (1,376 × 1,040 pixel) CCD camera (SensiCam-QE, Cooke Corp.). The CCD camera and the double-pulsed Nd:YAG laser were connected to a workstation (host computer) via a Digital Delay Generator (Berkeley Nucleonics, Model 565), which controlled the timing of the laser illumination and image acquisition. In the present study, the scaling factor of the acquired micro-PIV images was found to be 0.97 μm/pixel. After micro-PIV images were acquired, instantaneous PIV velocity vectors were obtained by a frame-to-frame cross-correlation technique involving successive frames of patterns of particle images in an interrogation window 32 × 32 pixels. An effective overlap of 50% of the interrogation windows was employed in PIV image processing. The measurement uncertainty level for the measurements of the instantaneous velocity vectors was estimated to be within 2.0%.

3 Experimental results and discussions

3.1 Characteristics of the unsteady micro-flow driven by the insulin pump

Figure 2 shows typical micro-PIV measurement results at four time instants when the focal plane of the microscopic objective (depth of field ~5.0 μm) was set to the midplane of the 300-μm-deep microchannel. The transient behavior of the unsteady micro-flow driven by the insulin pump was visualized clearly and quantitatively from the instantaneous flow velocity distributions. Based on the time sequences of the micro-PIV measurements, the histogram of the flow velocity variations in the center of the microchannel (i.e., streamwise-averaged centerline flow velocity) could be derived, which is given in Fig. 3. It can be seen clearly that the micro-flow inside the CSII tubing system was highly unsteady with the flow velocity changing significantly as a function of time. As expected, the period of the operation cycle of the insulin pump was found to be 180 s when the insulin pump was set at 2.0 U/H basal rate. During each insulin pump operation cycle, the centerline flow velocity was found to be very small for most of the time, except within the short time period when the insulin pump operated. The time-averaged centerline velocity over each insulin pump operation cycle was also plotted in the figure as the red dash line for comparison. It can be seen clearly that the behavior of the micro-flow inside the CSII tubing system is much more interesting than a creeping flow that the nominal time-averaged flow velocity would suggest. While the time-averaged centerline velocity was only about

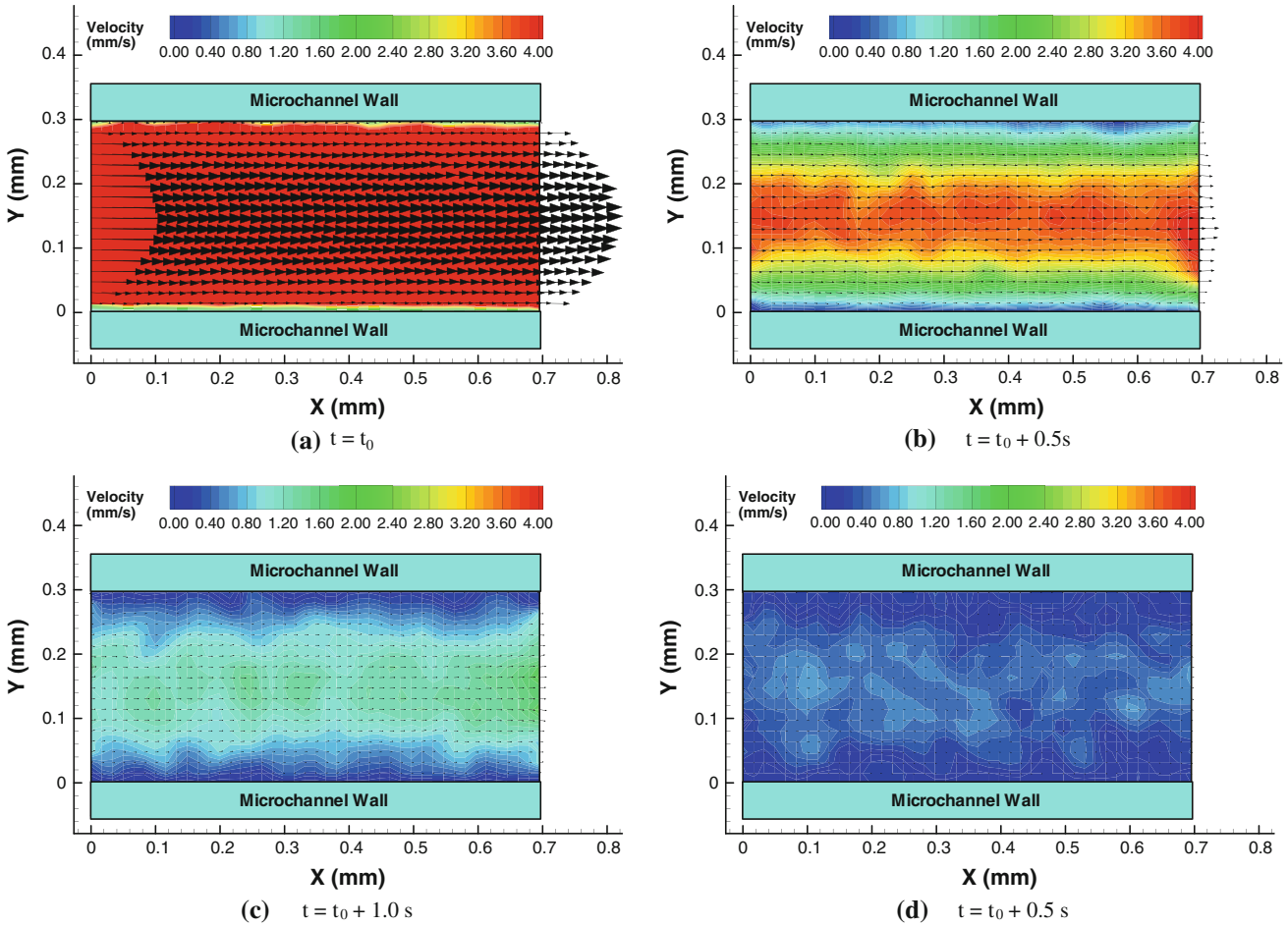

Fig. 2 Instantaneous velocity distributions inside the microchannel at 2.0 U/H basal rate

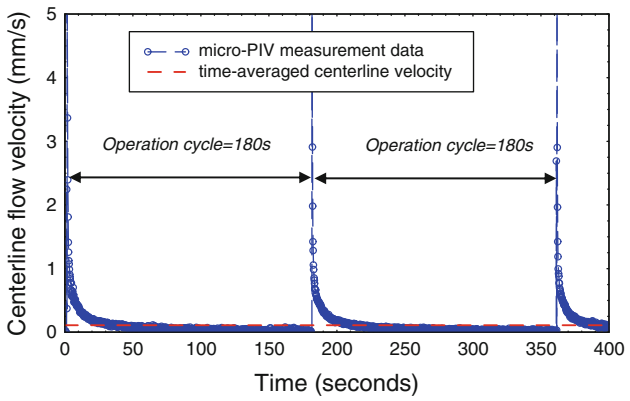

Fig. 3 Histogram of the centerline flow velocity at 2.0 U/H basal rate

0.098 mm/s (i.e., corresponding a creeping flow at the Reynolds number $Re_D = 0.030$), the maximum centerline flow velocity inside microchannel at the end of the insulin pump action pulse was found to be as high as 26.4 mm/s, which is more than 260 times higher than the time-averaged centerline flow velocity.

The dynamic response of the micro-flow inside the CSII tubing system upon the pulsed action of the insulin pump can be seen more clearly from the enlarged view of the centerline flow velocity variations before and after the action pulse of the insulin pump, which is given in Fig. 4. It can be seen clearly that while the period of the insulin pump operation cycle was 180 s at the basal rate of 2.0 U/H the real action time for the insulin pump was found to be only about 0.4 s. The short action time of 0.4 s estimated based on the micro-PIV measurements was found to agree well with the value reported by Demuren et al. (2009). As shown in Fig. 4, the flow velocity inside the microchannel was found to be very small, i.e., almost zero, before the action pulse of the insulin pump. A significant pressure head would be generated due to the pulsed action of the insulin pump. The flow velocity inside the infusion tubing system was found to increase rapidly as the insulin pump started to act. After the insulin pump action pulse ended, no additional pressure head would be generated to drive the micro-flow. As a result, the micro-flow inside the CSII tubing system was found to begin to decelerate and

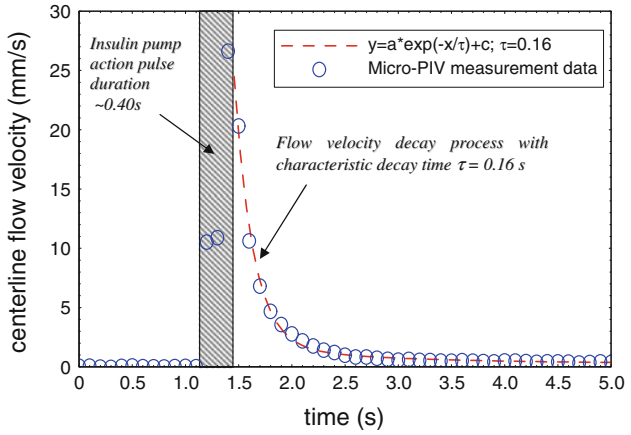

Fig. 4 Centerline flow velocity before and after an insulin pump action pulse

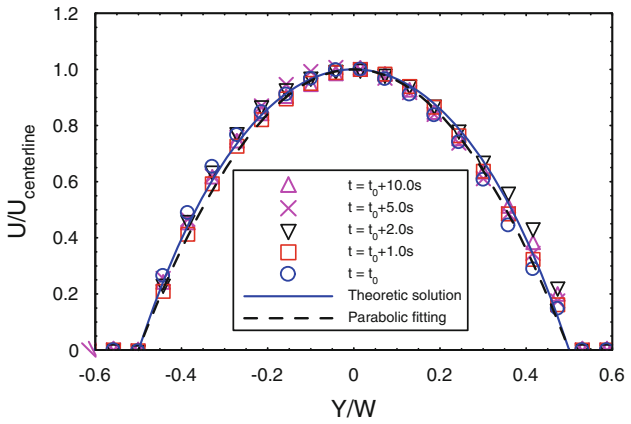

Fig. 5 Normalized flow velocity profiles at different time instants in the decay process

experience a flow decay process. As shown clearly in Fig. 4, the decay process of the centerline flow velocity inside the microchannel was found to be fitted reasonably well by an exponential function with the characteristic decay time, $\tau = 0.16$ s.

Figure 5 shows the normalized streamwise-averaged flow velocity profiles across the square microchannel at different time instants in the flow decay process after the pulsed action of the insulin pump. The time instant of $t = t_0$ corresponds to the end of the action pulse of the insulin pump. Surprisingly, although the magnitude of the flow velocity inside the microchannel was found to decrease rapidly in the flow decay process, the normalized flow velocity data (i.e., normalized by the maximum flow velocity at the centerline of the microchannel) at different time instants were found to align nicely in the plots. It indicates that the flow velocity profiles across the microchannel were self-similar during the flow decay process.

According to the textbook of White (1991), for a fully developed, pressure-driven laminar flow inside a rectangular channel of $-w \le z \le w$ and $-h \le y \le h$, the theoretical solution of the velocity distribution inside the rectangular channel can be expressed as:

$$U(y,z) = \frac{16h^2}{\mu\pi^3}\left(-\frac{dp}{dx}\right)\sum_{n=1,3,5\ldots}^{\infty}(-1)^{(n-1)/2} \left[1-\frac{\cosh(n\pi z/2w)}{\cosh(n\pi h/2w)}\right]\frac{\cosh(n\pi y/2h)}{n^3} \quad (1)$$

where w and h are the half width and half height of the rectangular channel, respectively. The term of $-\frac{dp}{dx}$ is the corresponding pressure gradient.

The theoretical solution given in Eq. 1 for a fully developed laminar channel flow as well as a parabolic curve fitting was also plotted in Fig. 5 for comparison. Interestingly, the measured velocity profiles across the microchannel were found to agree reasonably well with the theoretical solution for a fully developed laminar channel flow even though the micro-flow was still in transient state during the flow decay process.

In the present study, the micro-PIV measurements were also conducted at different depths of the square microchannel by adjusting the focal plane of the microscopic objective (depth of field $\sim$5.0 μm) along the depth direction of the square microchannel. Based on the PIV measurements at different channel depth, it was found that even though the absolute values of the flow velocity were found to become smaller and smaller as the measurement plane approaching either the top wall or the bottom wall of the microchannel the normalized velocity profiles at different channel depth are actually self-similar, which are shown in Fig. 6. The data shown in Fig. 6 were based on the same data reduction procedure as those shown in Fig. 5, but normalized by the local maximum flow velocity at each channel depth. The theoretical solution for a fully developed laminar channel flow as expressed by Eq. 1 and a

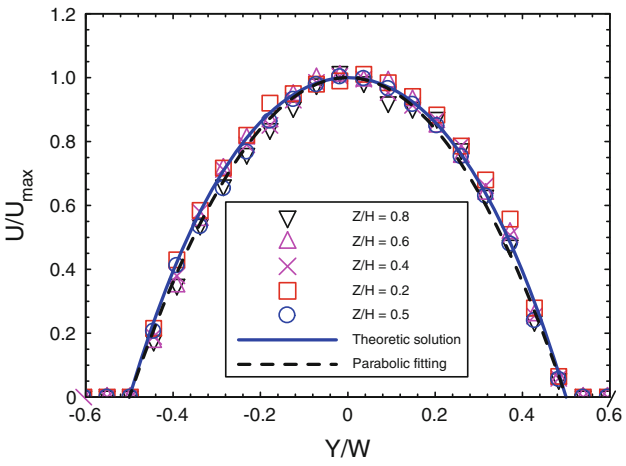

Fig. 6 Normalized flow velocity profiles at different channel depth

parabolic curve fitting were also plotted in the figure for comparison. It can be seen clearly that the normalized flow velocity distributions at different channel depths can also be represented reasonably well by the theoretical solution. In summary, the micro-PIV measurements suggest that the theoretical solution for a fully developed laminar channel flow expressed in Eq. 1 can be used to estimate the flow velocity distribution inside the square microchannel even though the micro-flow was in transient state during the flow decay process.

3.2 Effects of the air bubbles entrained inside the CSII tubing system

There are anecdotal evidences to show that air bubbles may be entrained into the tubing system of the CSII infusion set during the typical 3- to 5-day operation between refills. It has been suggested that air bubbles entrained into the micro-sized CSII tubing system may reduce or inhibit insulin delivery in CSII therapy. In the present study, an experimental study was also conducted to assess the effects of air bubbles entrained inside the micro-sized CSII tubing system on the insulin delivery. During the experiments, air bubbles were introduced into the CSII tubing system through the reservoir of the insulin pump. The behavior of the air bubbles inside the CSII tubing system upon the pulsed excitation of the insulin pump was monitored. The characteristic changes of the liquid micro-flow due to the air bubbles entrained inside the CSII tubing system were quantified based on the detailed flow field measurements using the micro-PIV technique.

By tracking the movement of the air bubbles inside the CSII tubing system, it was found that the air bubbles were pushed downstream along with the liquid fluid upon the pulsed action of the insulin pump. Eventually, the air bubbles were found to be expelled through the catheter of the infusion set along with the liquid fluid. As described above, the insulin pump was supposed to deliver the same amount (i.e., 1.0 μl) of the liquid fluid through the catheter during each action cycle. However, when air bubbles were entrained inside the CSII tubing system, the air bubbles were delivered by the insulin pump and expelled from the catheter along with the liquid fluid. As a result, the total amount of the liquid fluid actually delivered by the insulin pump was found to be much less than the pre-programmed value due to the existence of the air bubbles. It confirmed the conjecture that the air bubbles entrained into the CSII tubing system would reduce or even inhibit insulin delivery in CSII therapy. It should be noted that a large amount of the air bubbles entrained in the CSII tubing system may also cause the patient's life in danger due to the surplus mixing of gases in the blood (e.g., the caisson disease, decompression illness).

The micro-PIV measurements revealed more interesting features and underlying physics about the effects of air bubbles entrained into the CSII tubing system on the insulin delivery process. Figure 7 shows two typical micro-PIV measurement results of the flow velocity fields surrounding a small air bubble entrained inside the microchannel. As shown in the figure, the tip-to-tip length of the air bubble was about 450 μm (i.e., ~0.05 μl in volume). Cubaud et al. (2006) suggested that an air bubble traveling in a microchannel may lose their symmetry with respect to the center axis of the channel. As velocity increases, the advancing contact angle increases and the receding contact angle decreases. While the changes of the advancing and receding contact angles at the front and rear ends of the air bubble were not able to be distinguished easily from the acquired micro-PIV images shown in Fig. 7 due to the relatively low flow velocity of the present study, the measured flow velocity vectors around the air bubble reveal the significant changes in the flow features at the rear and front edges of the air bubble clearly. The liquid flow was found to be decelerated and diverge from the centerline along the interface at the rear end of the air bubble, while the liquid flow would be accelerated and converge toward the centerline at the front end. By using the air bubble as the frame of reference, the advancing tip of the air bubble would be a converging stagnation point, whereas the receding tip would be a diverging stagnation point, which agrees with the finding of Yamaguchi et al. (2009) in the study of the flow fields surrounding a migrating air bubbles inside a microchannel.

Figure 8 shows the micro-PIV measurement results near the front and rear ends of a relatively long air bubble entrained inside the CSII tubing system. The tip-to-tip length of the air bubble was found to be about 2.0 mm (i.e., ~0.2 μl in volume). Again, similar flow patterns can be observed around the long air bubble: the liquid flow would be decelerated and diverge from the centerline along the interface at the rear end of the air bubble and be accelerated and converge toward the centerline in the region near the front end of the air bubble. The PIV measurement results suggest that the deceleration/acceleration of the liquid flow at rear/front end of an air bubble is mainly influenced by the interfaces between the liquid and the air bubble, which is almost independent of size of the air bubble.

Based on the micro-PIV measurement results as those shown in Fig. 8, the normalized flow velocity profiles across the microchannel near the front and rear ends of the migrating air bubble were extracted, which were given in Fig. 9. It can be seen clearly that the flow velocity profiles in the regions near both rear and front ends of the air bubble were found to change significantly due to the existence of the air bubble. Outside the influential region (i.e., about 200 μm away from the front and rear ends of

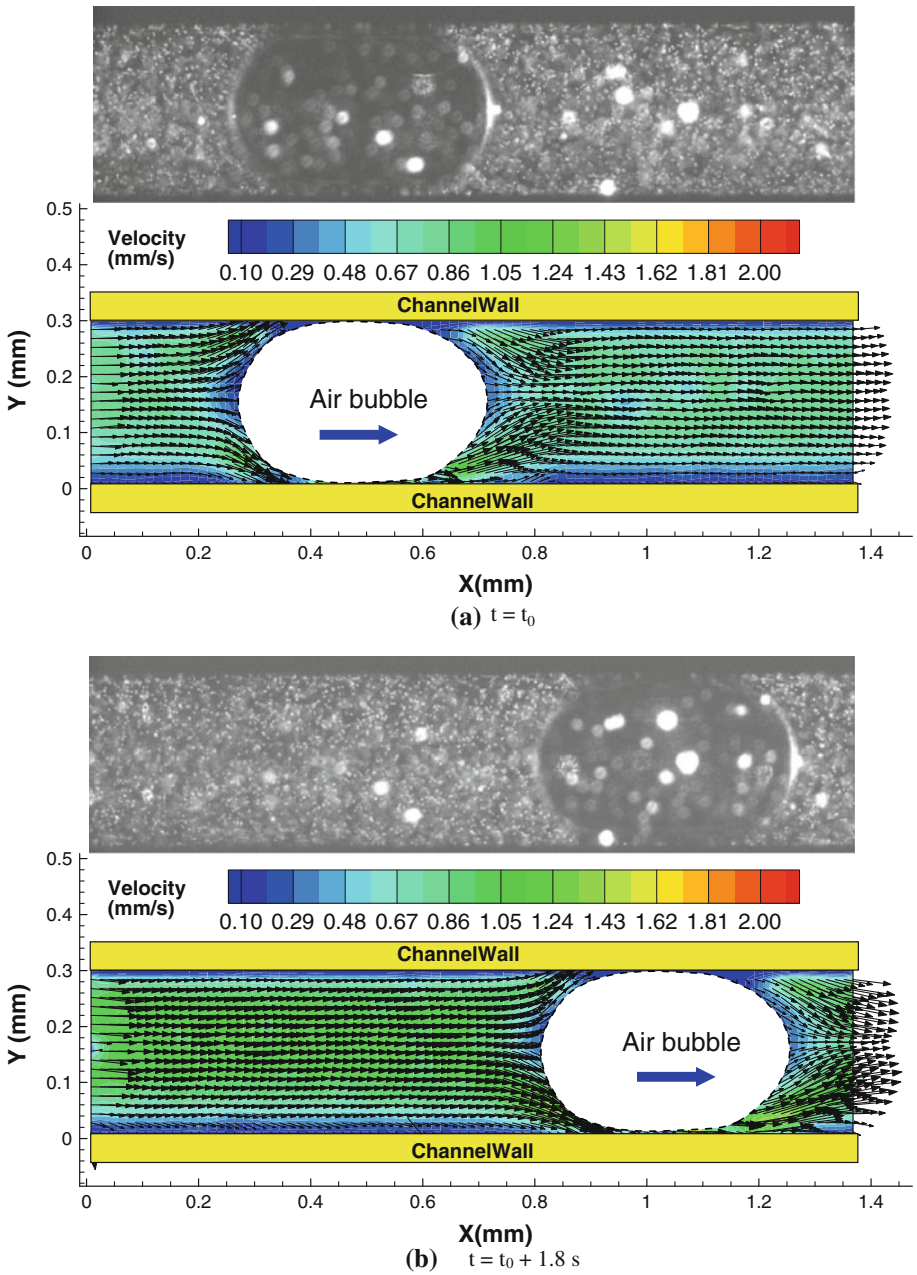

Fig. 7 Micro-PIV measurements around a small migrating air bubble inside the microchannel

the air bubble), the transverse flow velocity profiles were found to stay the same as those shown in Fig. 5 for the case without the air bubble, which can be represented reasonably well by the theoretical solution for a fully developed laminar channel flow expressed by Eq. 1. However, as the liquid flow approaching the rear end of the air bubble, the flow velocity was found to be decelerated and diverge from the channel centerline. As a result, the transverse velocity profiles were found to become much flat. Further toward the interface at the rear end of the air bubble, the flow velocity profiles were found to have apparent deficits in the middle region and two peaks at two sides near the corner regions. As described above, the liquid flow would be accelerated and converge toward the channel centerline in the region near the front end of the air bubble. The acceleration of the liquid flow near the front end of the air bubble can be seen very clearly from the transverse velocity profiles shown in Fig. 9b. Such measurement results were found to agree with those reported by Park et al. (2003), Miessner et al. (2008), and Yamaguchi et al. (2009) in the studies of two-phase flows in microchannels.

In addition to causing flow pattern changes in the regions near interfaces, the air bubbles inside the CSII tubing system were also found to significantly change the characteristics of the flow decay process after each action pulse of the insulin pump. As shown clearly in Fig. 10a, the

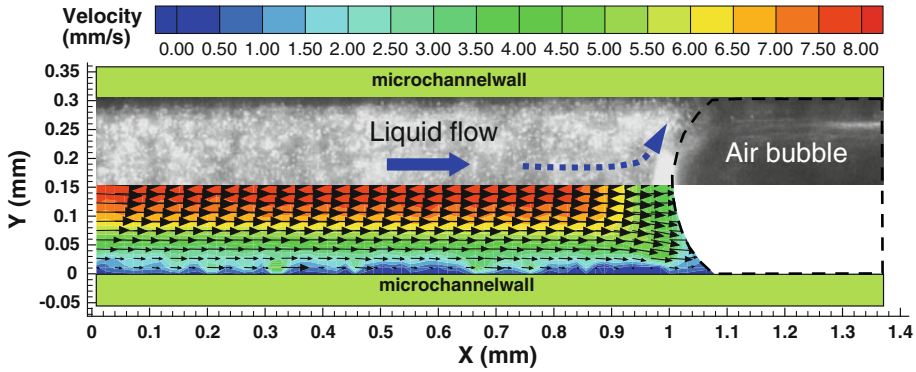

(a) near the rear end of the air bubble

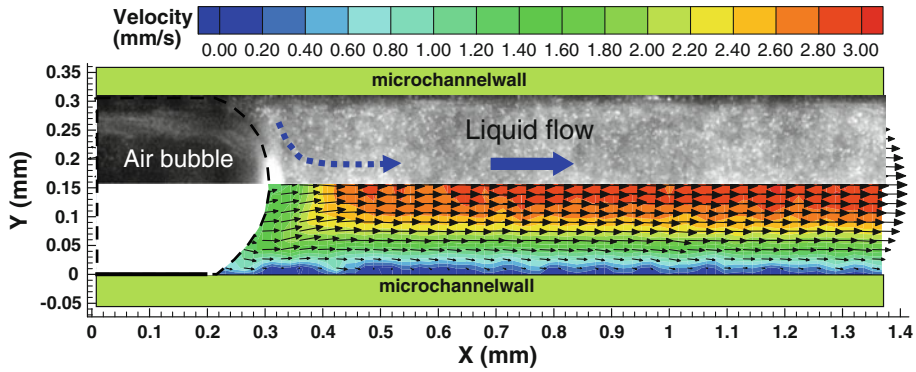

(b) near the front end of the air bubble

Fig. 8 Micro-PIV measurements near the rear and front ends of a long migrating air bubble

centerline flow velocity inside the microchannel would decay much more smoothly when no air bubbles were entrained in the CSII tubing system. For the case with air bubbles entrained inside the CSII tubing system, the decay curve was found to become much "noisier" with several "secondary humps" riding on the decay curve. This may be explained by the fact that the air bubbles entrained inside the CSII tubing system would act as shock absorbers to change the dynamic response of the micro-flow upon the pulsed action of the insulin pump. While the liquid flow is incompressible, the air bubbles are easily compressed and deformed when the wave front of the tremendous pressure head generated by the pulsed action of the insulin pump approaching the air bubbles. As the pressure wave front passed, the compressed air bubbles would stretch/expand to adjust the pressure difference across the air bubbles. As a result, the velocity decay process of the liquid flow would be affected by the compression and expansion of the air bubbles inside the CSII tubing system. The expansion of the compressed air bubbles could generate small pressure head to accelerate the liquid flow downstream of the air bubbles, which would result in the "secondary humps" riding on the decay curve as shown in Fig. 10a.

It was also found that the initial flow decay after the pulsed action of the insulin pump would become much slower due to the existence of the air bubbles entrained inside the CSII tubing system. As shown clearly in Fig. 10b, while the initial flow decay for the case with air bubble entrained inside the CSII tubing system can still be fitted reasonably well by using an exponential function, the characteristic decay time, τ, was found to increase greatly from $\tau = 0.16$ s for the case without air bubbles to $\tau = 0.31$ s for the case with $a \sim 5.0$-mm-long air bubble (i.e., 5.0 μl in volume) entrained inside the CSII tubing system. The significant change (i.e., almost doubled the value) of the characteristic decay time is believed to be closely related to the change in the compressibility of the micro-flow due to the existence of the air bubbles inside the CSII tubing system. Compared with the case without air bubbles, the propagation speed of the pulsed pressure waves generated by the pulsed actions of the insulin pump would slow down greatly due to the compressible air bubbles inside the CSII tubing system. As a result, the initial flow decay after the pulsed action of the insulin pump would be retarded due to the existence of the air bubbles inside the CSII tubing system.

4 Concluding remarks

An experimental study was conducted to investigate the unsteady micro-flow driven by an insulin pump commonly used in continuous subcutaneous insulin infusion (CSII) therapy. A micro-PIV system was used to conduct

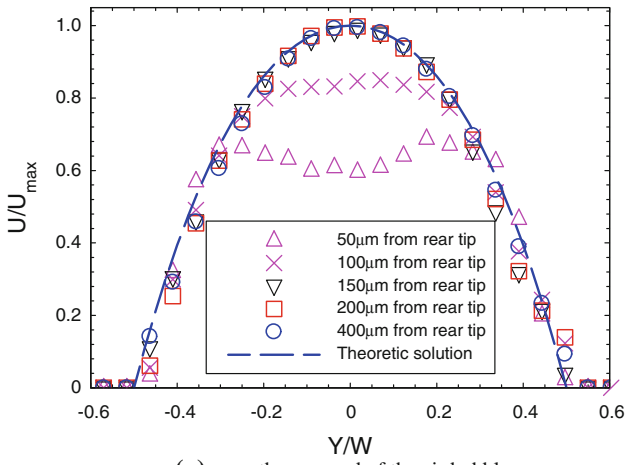

(a) near the rear end of the air bubble

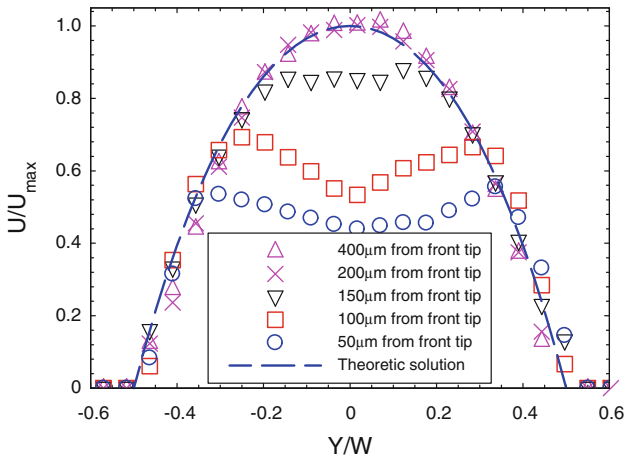

(b) near the front end of the air bubble

Fig. 9 Measured transverse velocity profiles near the rear and front ends of an air bubble

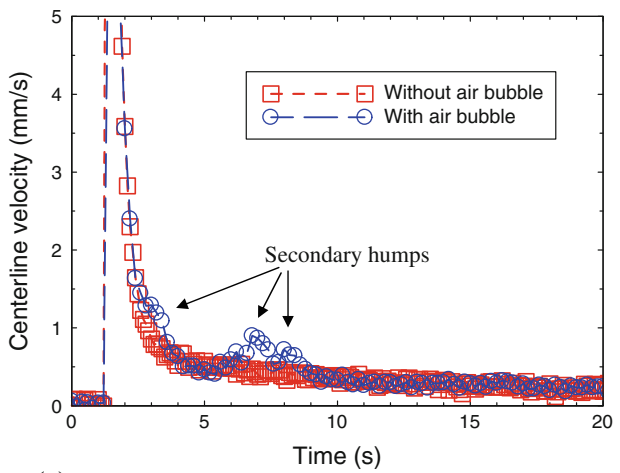

(a) The flow velocity decay curves with and without air bubble entrainment

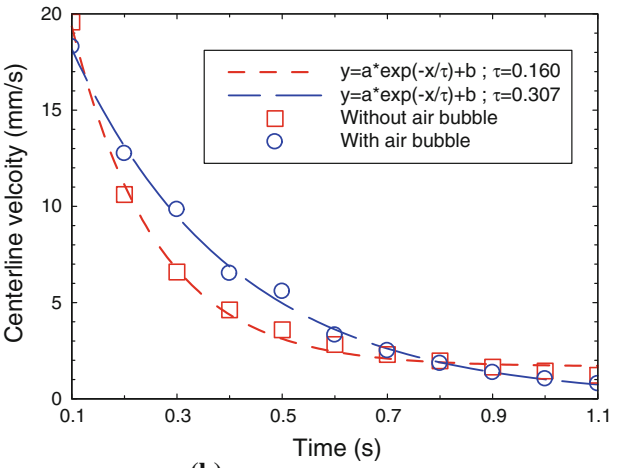

(b) Effects on the initial decay process

Fig. 10 Effects of the air bubble entrainment on the flow decay process

detailed flow velocity field measurements inside a 300 μm × 300 μm microchannel to characterize the transient behavior of the unsteady micro-flows upon the pulsed actuation of the insulin pump. It was found that the micro-flow driven by the insulin pump was highly unsteady, which is much more interesting than the creeping flow that the nominal averaged flow velocity would suggest. While the period of the operation cycle of the insulin pump was 180 s at the basal rate of 2.0 U/H, the real action time of the insulin pump was found to be only about 0.4 s. Tremendous pressure head would be generated within the short pulse to push the liquid flow from the reservoir of the insulin pump to the CSII tubing system for insulin delivery. As a result, the flow velocity inside the infusion tubing system was found to vary significantly during the operation cycle of the insulin pump. As the insulin pump started to operate, the flow velocity within the CSII tubing system was found to increase rapidly. The centerline flow velocity was found to reach 26.4 mm/s at the end of the insulin pump action pulse, which is about 260 times higher than the time-averaged flow velocity during each insulin pump operation cycle. The flow velocity within the CSII tubing system was found to decrease swiftly after each pulsed action of the insulin pump. The decay process of the flow velocity was found to be represented well by an exponential function with the characteristic decay time of 0.16 s. Interestingly, although the magnitude of the flow velocity inside the infusion tubing system was found to decrease rapidly during the flow decay process, the velocity distributions of the micro-flow at different time instants were found to be self-similar. The normalized flow velocity profiles across the microchannel were found to fit reasonably well by the theoretical solution of a fully developed laminar channel flow even though the micro-flow was in transient state during the decay process.

An experimental study was also conducted to assess the effects of the air bubbles entrained inside the CSII tubing system on the insulin delivery. The micro-PIV measurements revealed clearly that the flow patterns of the micro-flow inside the CSII tubing system would be changed dramatically in the regions near the interfaces between the liquid fluid and the air bubbles. The liquid flow was found to be decelerated and diverge along the interfaces at the rear ends of the migrating air bubbles, whereas the liquid flow at the front ends of the air bubbles would be accelerated and converge toward the channel centerline. It was also found that the total amount of the liquid fluid delivered by the insulin pump through the catheter of the infusion set would become much less than the pre-programmed value due to the existence of the air bubbles inside the CSII tubing system. In addition to reducing the total amount of the liquid fluid delivered by the insulin pump, the air bubbles were also found to act as shock absorbers to change the dynamic response of the micro-flow upon the pulsed action of the insulin pump. Besides the fact that the flow velocity decay curve would become much "noisier" with several "secondary humps" riding on the decay curve, the initial flow decay after the pulsed action of the insulin pump was found to be retarded greatly (i.e., the characteristic decay time become much longer) due to the existence of the air bubbles inside the CSII tubing system.

Acknowledgments The authors also want to thank Dr. Zheyan Jin of Iowa State University for his help in setting up the micro-PIV experiments. The support of National Science Foundation CAREER program under award number of CTS-0545918 is gratefully acknowledged.

References

Alemzadeh R, Ellis JN, Holzum MK, Parton EA, Wyatt DT (2004) Beneficial effects of continuous subcutaneous insulin infusion and flexible multiple daily insulin regimen using insulin glargine in type 1 diabetes. Pediatrics 114(1):91–95

Bruttomesso D, Costa S, Baritussio A (2009) Continuous subcutaneous insulin infusion (CSII) 30 years later: still the best option for insulin therapy. Diabetes Metab Res Rev 25:99–111

Cubaud T, Ulmanella U, Ho CM (2006) Two-phase flow in microchannels with surface modifications. Fluid Dyn Res 38:772–786

Demuren A, Doane S (2007) A study of insulin occlusion using the medtronic minimed paradigm 511 insulin pump. ODU Research Foundation Project Report

Demuren A, Gyuricsko E, Diawara N, Castro N, Carter J, Bhaskara R (2009) Impaired insulin delivery during continuous subcutaneous insulin infusion. Report to ODU Research Office 2009 Seed Grant

Gallardo BS, Gupta VK, Eagerton FD, Jong LI, Craig VS (1999) Electrochemical principles for active control of liquids on submillimeter scales. Science 283:57–60

Hartman I (2008) **I**nsulin analogs: impact on treatment success, satisfaction, quality of life, and adherence. Clin Med Res 6(2):54–67. doi:10.3121/cmr.2008.793

Johnson RD, Badr IHA, Barrett G, Lai S, Lu Y (2001) Development of a fully integrated analysis system for ions based on ion-selective optodes and centrifugal microfluidics. Anal Chem 73: 3940–3946

Kim MJ, Beskok A, Kihm KD (2002) Electro-osmosis-driven microchannel flows: a comparative study of microscopic particle image velocimetry measuremens and numerical simulations. Exp Fluids 33:170–180

Kinoshita H, Kaneda S, Fujii T, Oshima M (2007) Three-dimensional measurement and visualization of internal flow of a moving droplet using confocal micro-PIV. Lab Chip 7:338–346

Li H, Olsen GM (2006) MicroPIV measurements of turbulent flow in square microchannels with hydraulic diameters from 200 μm to 640 μm. Int J Heat Fluid Flow 27:123–134

Meinhart CD, Wereley ST, Santiago JG (1999) PIV measurements of a microchannel flow. Exp Fluids 27:414–419

Miessner U, Lindken R, Westerweel J (2008) 3D-velocity measurements in microscopic two-phase flows by means of micro-PIV. In: 14th int symp on applications of laser techniques to fluid mechanics

Olsen MG, Bourdon CJ (2003) Out-of-plane motion effects in microscopic particle image velocimetry. ASME J Fluids Eng 125:895–901

Park JS, Choi CK, Kihm KD, Allen JS (2003) Optically-sectioned PIV measurements using CLSM. J Heat Transf 125(4):542

Poulsen C, Langkjaer L, Worsoe C (2005) Precipitation of insulin products used for continuous subcutaneous insulin infusion. Diabetes Technol Ther 7(1):142–150

Prins MWJ, Welters WJJ, Weekamp JW (2001) Fluid control in multichannel structures by electrocapillary pressure. Science 291:277–280

Rossetti P, Porcellati F, Fanelli CG, Perriello G, Torlone E, Bolli GB (2008) Superiority of insulin analogues versus human insulin in the treatment of diabetes mellitus. Arch Physiol Biochem 114(1):3–14

Santiago JG, Wereley ST, Meinhart CD, Beebe DJ, Adrian RJ (1998) A micro particle image velocimetry system. Exp Fluids 25:316–319

Shalitin S, Phillip M (2008) The use of insulin pump therapy in the pediatric age group. Horm Res 70:14–21

Weissberg-Benchell J, Goodman SS, Lomaglio JA, Zebracki K (2007) The use of continuous subcutaneous insulin infusion (CSII): parental and professional perceptions of self-care mastery and autonomy in children and adolescents. J Pediatr Psychol 32(10):1196–1202

White F (1991) Viscous fluid flow, 2nd edn. Mcgraw-Hill, New York

Wolpert HA, Faradji RN, Bonner WS, Lipes MA (2002) Metabolic decompensation in pump users due to lispro insulin precipitation. BMJ 324:1253

Yamaguchi E, Smith BJ, Gaver DP (2009) μ-PIV measurements of the ensemble flow fields surrounding a migrating semi-infinite bubble. Exp Fluids 47:309–320